Error Performance of NOMA VLC Systems

Hanaa Marshoud*, Paschalis C. Sofotasios*,†, Sami Muhaidat*,‡, George K. Karagiannidis§ and Bayan S. Sharif*

*Department of Electrical and Computer Engineering, Khalifa University, United Arab Emirates
e-mail: {hanaa.marshoud; bayan.sharif}@kustar.ac.ae
†Department of Electronics and Communications Engineering, Tampere University of Technology, Finland
e-mail: p.sofotasios@ieee.org
‡Department of Electronic Engineering, University of Surrey, United Kingdom
e-mail: muhaidat@ieee.org
§Department of Electrical and Computer Engineering, Aristotle University of Thessaloniki, Greece
e-mail: geokarag@auth.gr

***Abstract*—Visible light communication (VLC) systems are expected to provide remarkably high speed indoor communications and effective ubiquitous connectivity. However, the key limitation of such systems is the narrow modulation bandwidth of the light sources. Based on this, non-orthogonal multiple access (NOMA) has been recently proposed as an effective method that can enhance considerably the spectral efficiency of indoor downlink VLC systems. In this context, the present work is devoted to the evaluation of the bit-error-rate (BER) performance of NOMA-based VLC systems. Specifically, a novel closed-form expression is first derived for the BER of the considered set up, by also taking into account the realistically incurred cancellation errors and interference terms. The validity of the derived expressions is verified through extensive comparisons with respective results from Monte Carlo simulations, while their algebraic representation is relatively simple, which renders them convenient to handle both analytically and numerically. This leads to meaningful insights on the behavior and performance gains achieved, thanks to the adoption of NOMA, which are particularly useful in future design and deployment of VLC systems.**

I. Introduction

Visible light communication (VLC) has recently emerged as a promising and efficient solution to indoor ubiquitous broadband connectivity [1]. Motivated by this, several multiple access schemes have been adopted to enhance the achievable throughput in high-rate VLC downlink networks, including, carrier sense multiple access (CSMA), orthogonal frequency division multiple access (OFDMA), code division multiple access (CDMA) and time division multiple access (TDMA) [2]. In this context, non-orthogonal multiple access (NOMA) was proposed in [3] as a spectrum-efficient power-domain based multiple access scheme for downlink VLC systems.

It is recalled that the signals of different users in NOMA systems are fundamentally superimposed in the power domain by allocating different power levels based on the channel conditions of each user. Therefore, users can share the entire frequency and time resources leading to increased spectral efficiency. It is also recalled that NOMA is based on allocating higher power levels to users with worse channel conditions compared to those with favorable channel conditions. As a result, the user with the highest allocated power is ultimately rendered capable of directly decoding its signal, while treating the signals of other users as noise. Meanwhile, the rest of the users in the system attempt to mitigate the corresponding resulting interference, by performing successive interference cancellation (SIC) for the multi-signal separation, prior to decoding their signals.

The performance of NOMA-based VLC systems has attracted a vast interest and few investigations have been recently reported. Specifically, NOMA-VLC was analyzed in [4] and [5] in terms of coverage probability and ergodic sum rate, where it was shown that NOMA can provide capacity gains compared to those achieved by TDMA. Likewise, it was also shown in [6] that NOMA outperforms OFDMA in terms of the achievable data rate in the downlink of VLC systems. Motivated by this, the present analysis considers NOMA as a multiple access scheme for the downlink of indoor VLC networks. This is based on the fact that it can provide certain advantages including: 1) NOMA is efficient in multiplexing a small number of users, which is the case in VLC sytems where a light-emitting diode (LED) is regarded as a small cell that serves few users in room environments; 2) NOMA provides superior performance gains at high signal-to-noise (SNR) scenarios [7]. This makes it particularly suitable for VLC links, as they typically operate at rather high SNR values thanks to the existence of strong line-of-sight (LOS) components and short propagation distances.

In this context, we investigate the error performance of NOMA-VLC systems by deriving an exact and rather simple analytic expression for the corresponding bit-error-rate (BER), for the case of arbitrary number of users. It is noted that, to the best of our knowledge, this is the first work that investigates the BER performance of NOMA-based systems, including similar analyses in conventional radio communication scenarios.

The remainder of the paper is organized as follows: Section II describes the channel and system model of an indoor VLC downlink network. Section III is then devoted to the error analysis of NOMA-VLC systems while numerical results and related discussions are presented in Section IV. Finally, closing remarks are provided in Section V.

978-1-4673-8999-0/17/$31.00 ©2017 IEEE

II. Channel and System Model

We consider a single-LED downlink VLC system deployed in a regular indoor environment. The LED has a dual function of illumination and communication, and serves N users simultaneously by modulating the intensity of the emitted light according to the data received through a power line communications backbone network. Furthermore, all users are assumed to be equipped with a single photo-detector (PD) that performs direct detection in order to extract the transmitted signal from the received optical carrier. This is practically realized by means of unipolar on-off keying (OOK) modulation, which is considered thanks to its effectiveness in VLC systems, which in fact renders it a rather popular option [8], [9] and the references therein.

A. The VLC Channel

The considered communication set up is based on LOS communication scenarios as illustrated in Fig. 1, since multipath delays resulting from incurred reflections and diffuse refractions are typically negligible in indoor VLC settings [10]. To this effect, the wireless channel between user U_i and the corresponding LED can be represented as follows:

$$h_i = \begin{cases} \frac{A_i}{d_i^2} R_o(\varphi_i) T_s(\phi_i) g(\phi_i) \cos(\phi_i), & 0 \le \phi_i \le \phi_c \\ 0, & \phi_i > \phi_c \end{cases} \quad (1)$$

where i =1, 2, 3, …,N, A_i denotes the receiver PD area, d_i accounts for the distance between the transmitting LED and the *i*-th receiving PD, φ_i is the angle of emergence with respect to the transmitter axis, ϕ_i is the angle of incidence with respect to the receiver axis, ϕ_c is the field of view (FOV) of the PD, $T_s(\phi_i)$ is the gain of optical filter and $g(\phi_i)$ is the gain of the optical concentrator, which is expressed as

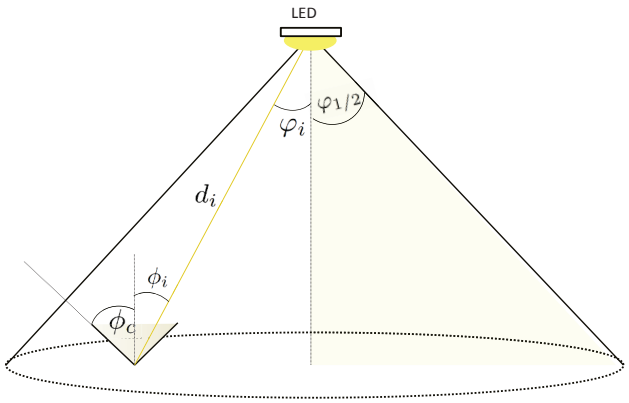

Figure 1: VLC channel model.

$$g(\phi_i) = \begin{cases} \frac{n^2}{\sin^2(\phi_c)}, & 0 \le \phi_i \le \phi_c \\ 0, & \phi_i > \phi_c \end{cases} \quad (2)$$

where n denotes the corresponding refractive index. Moreover, $R_o(\varphi_i)$ in (1) is the Lambertian radiant intensity of the transmitting LEDs, which can be expressed as

$$R_o(\varphi_i) = \frac{m+1}{2\pi} \cos^m(\varphi_i) \quad (3)$$

where m is the order of Lambertian emission, calculated as

$$m = -\frac{\ln(2)}{\ln(\cos(\varphi_{1/2}))} \quad (4)$$

with $\varphi_{1/2}$ denoting the transmitter semi-angle at half power. Based on this, the receiver-site noise is drawn from a circularly-symmetric Gaussian distribution of zero mean and variance, namely

$$\sigma_n^2 = \sigma_{sh}^2 + \sigma_{th}^2 \quad (5)$$

where σ_{sh}^2 and σ_{th}^2 denote the variances of the shot noise and thermal noise, respectively.

The shot noise in optical wireless channels results from the high rate physical photo-electronic conversion process, with variance at the *i*-th PD given by

$$\sigma_{sh_i}^2 = 2qB\left(\gamma h_i x_j + I_{bg} I_2\right) \quad (6)$$

where q represents the electronic charge, γ is the detector responsivity, B is the corresponding bandwidth, I_{bg} is background current, and I_2 is the noise bandwidth factor. Furthermore, the thermal noise is generated within the transimpedance receiver circuitry and its variance is given by

$$\sigma_{th_i}^2 = \frac{8\pi K T_k}{G} \eta A I_2 B^2 + \frac{16\pi^2 K T_k \Gamma}{g_m} \eta^2 A^2 I_3 B^3 \quad (7)$$

where K is Boltzmann's constant, T_k is the absolute temperature, G is the open-loop voltage gain, A is the PD area, η is the fixed capacitance of the PD per unit area, Γ is the field-effect transistor (FET) channel noise factor, g_m is the FET transconductance, and I_3 = 0.0868 [11].

B. NOMA Transmission

As already mentioned, NOMA is a recently introduced power-domain multiple access scheme that constitutes an effective strategy for providing significant performance gains in emerging communication systems. In the considered scenario and without loss of generality, we assume that the users $U_1, \ldots, U_N$ are sorted in an ascending order according to their channels, i.e. $h_1 \le h_2 \le \cdots \le h_N$. Based on the proposed NOMA concept, the corresponding LED transmits the real and non-negative signals $s_1, \ldots, s_N$ with associated power values $P_1, \ldots, P_N$, where s_i conveys information intended for user U_i, as shown in Fig. 2. It is also noted here that, unless otherwise stated, the term power refers to the corresponding optical power which is directly proportional to the LED driving current. To this effect, the N transmitted signals are superimposed in the power domain as

$$x = \sum_{i=1}^{N} P_i s_i \quad (8)$$

and the corresponding LED total transmit power is given by

$$P_{\text{LED}} = \sum_{i=1}^{N} P_i. \quad (9)$$

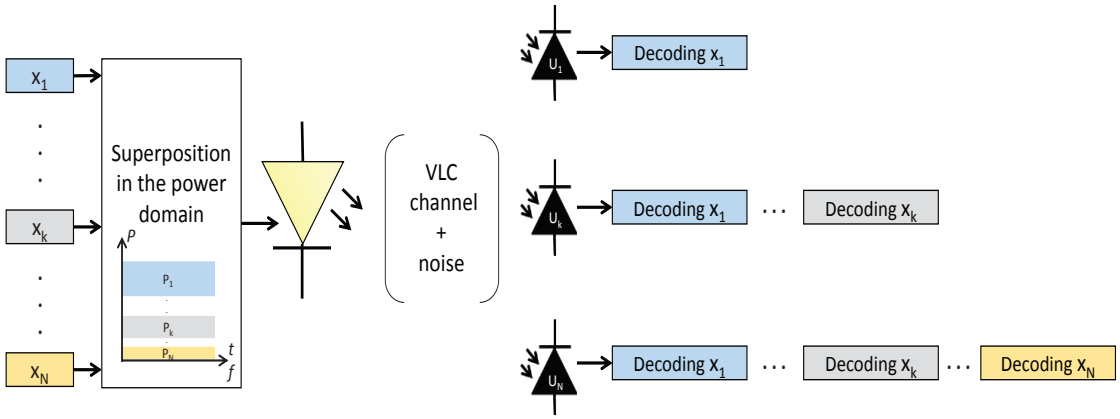

Figure 2: Representation of a NOMA-VLC downlink.

At the PD site, direct detection of the received signal is performed based on the received optical power. The received signal at user U_k can be expressed as

$$y_k = \gamma h_k \sum_{i=1}^{N} P_i s_i + n_k \tag{10}$$

where γ is the detector responsivity and n_k denotes zero-mean additive white Gaussian noise (AWGN) with variance σ_n^2. Henceforth, the $\mathcal{N}(\mu, \sigma^2)$ notation represents the probability density function (PDF) of Gaussian distribution with mean μ and variance σ^2.

Based on this and assuming unipolar OOK signals, the PDF of the received signal at U_k can be represented as

$$\begin{cases} f_{Y_k|S_k}(y_k|s_k=0) = \mathcal{N}_{y_k}(\gamma h_k \sum\limits_{\substack{i=1 \\ i\neq k}}^{N} P_i s_i, {\sigma_n}^2) \\ f_{Y_k|S_k}(y_k|s_k=1) = \mathcal{N}_{y_k}(\gamma h_k (P_k + \sum\limits_{\substack{i=1 \\ i\neq k}}^{N} P_i s_i), {\sigma_n}^2). \end{cases} \tag{11}$$

It is recalled here that the multi-user interference at user U_k can be eliminated by means of SIC. Based on this, in order to decode its own signal, U_k needs to successfully decode and subtract the signals of all other users with lower decoding order, i.e. $s_1, \ldots, s_{k-1}$. As a result, the residual interference from $s_{k+1}, \ldots, s_N$ becomes insignificant and can be treated as noise. Also, in order to facilitate SIC decoding, the LED allocates higher transmission power to users with poor channel gains. To this effect, the simplest power allocation scheme is the fixed power allocation (FPA), where the associated power of the *i*-th sorted user is set to

$$P_i = \rho P_{i-1} \tag{12}$$

with ρ denoting the power allocation factor ($0 < \rho < 1$). According to FPA in the context of the NOMA concept, the power allocated to user U_i is reduced at increase of h_i because users with good channel conditions require lower power levels to successfully decode their desired signals, after canceling the interference from the signals of the users with lower decoding order. This is, in fact, the fundamental principle of NOMA, which has been also shown to provide considerable performance gains in conventional radio communications [12].

III. Error Rate Analysis of NOMA-VLC Systems

In this section, we derive a closed form expression for the BER of a NOMA-based VLC system employing unipolar OOK under the assumption of perfect knowledge of the channel coefficients and ideal time synchronization.

Theorem 1. *Given that user U_k attempts to cancel the first $k-1$ signals from the aggregate received signal in succession, the BER of U_k in the NOMA scheme can be expressed as*

$$\begin{aligned} \mathrm{Pr}_{\mathrm{e_k}} = & \sum_{\mathrm{e_{k-1}}=-1,0,1} \cdots \sum_{\mathrm{e_1}=-1,0,1} \mathcal{P}(\mathrm{e_{k-1}}|\mathrm{e_1}, \ldots, \mathrm{e_{k-2}}) \\ & \times \mathcal{P}(e_{k-2}|e_1, \ldots, e_{k-3}) \times \cdots \times \mathcal{P}(e_1) \times \mathrm{Pr}_{\mathrm{e_k}}|\mathrm{e_1}, \ldots, \mathrm{e_{k-1}} \end{aligned} \tag{13}$$

where

$$\mathcal{P}(e_i|e_1, \ldots, e_{i-1}) = \begin{cases} 1 - \mathrm{Pr}_{e_i|e_1,\ldots,e_{i-1}} & e_i = 0 \\ \frac{1}{2}\mathrm{Pr}_{e_i|e_1,\ldots,e_{i-1}} & e_i = -1, 1 \end{cases}$$

with $e_i = \hat{s_j} - s_j$ denoting the error in detecting the i*-th OOK signal. Furthermore, $\mathrm{Pr}_{\mathrm{e_k}}|\mathrm{e_1}, \ldots, \mathrm{e_{k-1}}$ is the error probability in decoding the* k*-th signal conditioned on the previous detections, namely*

$$\begin{aligned} & \mathrm{Pr}_{e_k}|e_1, \ldots, e_{k-1} = \\ & \frac{1}{2^{N-k+1}} \sum_{i=1}^{2^{N-k}} \mathcal{Q}\left(\frac{\gamma h_k}{\sigma_n} \left(\frac{P_k}{2} - \sum_{j=1}^{k-1} e_j P_j - \sum_{l=k+1}^{N} P_l A_{il} \right) \right) \\ & + \frac{1}{2^{N-k+1}} \sum_{i=1}^{2^{N-k}} \mathcal{Q}\left(\frac{\gamma h_k}{\sigma_n} \left(\frac{P_k}{2} + \sum_{j=1}^{k-1} e_j P_j + \sum_{l=k+1}^{N} P_l A_{il} \right) \right) \end{aligned} \tag{14}$$

where $\mathcal{Q}(x) \triangleq \frac{1}{\sqrt{2\pi}} \int_x^\infty e^{-\frac{y^2}{2}} dy$ *denotes the one dimensional Gaussian* $Q-$*function and* $\sum_{j=1}^{k-1} e_j P_j$ *represents the potential residual interference caused by detection error in the decoding of* $s_1, \ldots, s_{k-1}$*. Moreover,* $\sum_{l=k+1}^{N} P_l A_{il}$ *corresponds to the interference caused by* $s_{k+1}, \ldots, s_N$*, where the elements of the matrix*

$$\boldsymbol{A} = \begin{bmatrix} A_{1\ k+1} & \cdots & A_{1\ N} \\ A_{2\ k+1} & \cdots & A_{2\ N} \\ \vdots & \vdots & \vdots \\ A_{2^{N-k}\ k+1} & \cdots & A_{2^{N-k}\ N} \end{bmatrix} = \begin{bmatrix} 0 & 0 & \ldots & 0 \\ 0 & 0 & \ldots & 1 \\ \vdots & \vdots & \vdots & \vdots \\ 1 & 1 & \ldots & 1 \end{bmatrix} \tag{15}$$

demonstrate the possible combinations of interference depending on the transmitted OOK vectors. □

Proof. Using maximum-likelihood (ML) detector, the decoder at the *k*-th receiver decides for the vector $\hat{s}$ that minimizes the Euclidean distance between the received signal vector y and the potential received signals, leading to

$$\hat{s} = \arg\min_{s} |y - \gamma h_k P_k s|^2 . \tag{16}$$

Based on this and assuming that the U_k user cancels successfully the signals s_1 , …, s_{m-1}, the error probability at U_k in detecting the signal s_m intended to user U_m $(1 \leq m \leq k-1)$ can be expressed as follows: when the transmitted symbol $s_m = 0$, the conditional error probability is given by

$$\Pr_{e_{m\to k|s_m=0}} = \int_{\frac{1}{2}\gamma h_k P_m}^{\infty} \mathcal{N}_{y_k}\left(\gamma h_k \sum_{i=m+1}^{N} P_i s_i, \sigma_n\right) dy_k \tag{17}$$

which can be expressed in closed-form in terms of the one dimensional Gaussian $Q-$function, namely

$$\Pr_{e_{m\to k|s_m=0}} = \mathcal{Q}\left(\frac{\gamma h_k}{\sigma_n}\left(\frac{P_m}{2} - \sum_{i=m+1}^{N} P_i s_i\right)\right). \tag{18}$$

On the contrary, when $s_m = 1$ is transmitted, it follows that

$$\Pr_{e_{m\to k|s_m=1}} = \int_{-\infty}^{\frac{1}{2}\gamma h_k P_m} \mathcal{N}_{y_k}\left(\gamma h_k \left(P_m + \sum_{i=m+1}^{N} P_i s_i\right), \sigma_n\right) dy_k \tag{19}$$

which after some algebraic manipulations, it can be expressed by the following closed-form expression

$$\Pr_{e_{m\to k|s_m=1}} = 1 - \mathcal{Q}\left(\frac{\gamma h_k}{\sigma_n}\left(-\frac{P_m}{2} - \sum_{i=m+1}^{N} P_i s_i\right)\right). \tag{20}$$

To this effect and by recalling the standard identity $Q(-x) = 1 - Q(x)$, the above representation can be equivalently re-written as follows:

$$\Pr_{e_{m\to k|s_m=1}} = \mathcal{Q}\left(\frac{\gamma h_k}{\sigma_n}\left(\frac{P_m}{2} + \sum_{i=m+1}^{N} P_i s_i\right)\right). \tag{21}$$

It is noted here that the above expressions assume perfect cancellation of the first $m-1$ signals. Nevertheless, detection errors may practically occur at any stage of the successive cancellation process. Therefore, considering the contribution of the residual interference inherited by cancellation errors, equations (18)-(19) can be alternatively re-written according to (22) and (23), at the top of the next page, which are expressed in closed-form by the following, easily computed explicit expressions

$$\Pr_{e_{m\to k|s_m=0}} = \mathcal{Q}\left(\frac{\gamma h_k}{\sigma_n}\left(\frac{P_m}{2} - \Upsilon - \sum_{i=m+1}^{N} P_i s_i\right)\right) \tag{24}$$

and

$$\Pr_{e_{m\to k|s_m=1}} = \mathcal{Q}\left(\frac{\gamma h_k}{\sigma_n}\left(\frac{P_m}{2} + \Upsilon + \sum_{i=m+1}^{N} P_i s_i\right)\right) \tag{25}$$

respectively. In the above representations, $\Upsilon = \sum_{j=1}^{m-1} e_j P_j$ denotes the cancelation errors in the previous detections. Therefore, it is evident that the total error probability in decoding s_k at U_k can be finally obtained by summing up all conditional error probabilities of the previous detections, which completes the proof. □

As already mentioned, the derived analytic expressions are novel and have a relatively simple algebraic representation that renders them convenient to handle both analytically and numerically, as they can be readily computed with the aid of popular software packages.

IV. Numerical Results and Discussion

In this section, we employ the derived analytic expressions to evaluate the performance of the considered VLC system setup. Respective results from extensive Monte Carlo simulations are also provided to verify the validity of the analytical results. The BER performance of a NOMA-VLC downlink system is analyzed for different scenarios based on the system and channel model in Section II. To this end and without loss of generality, we consider a $4m \times 4m \times 3m$ room with one transmitting LED mounted at the centre of the ceiling. Furthermore, we assume the existence of three users in the coverage area of the transmitting LED that are served simultaneously using NOMA. It is emphasized here that this number of users is selected for indicative purposes and that the considered system model is generic and applicable to any number of users. In this context, the LED superimposes the signals of the three users in the power domain by allocating the power values P_1, P_2 and P_3 to U_1, U_2 and U_3 respectively, under the constraint $P_1 + P_2 + P_3 = P_{\text{LED}}$. In the used notation, U_i denotes the user in *i*-th decoding order; that is, h_i is in the *i*-th ascending order of the channel gains. If not otherwise specified, the involved system parameters are set to the values depicted in Table I.

We evaluate the BER performance with regard to the transmit SNR in order to include the individual path gain of each user. Since the channel gain is in the order of 10^{-4}, the corresponding results exhibit an offset of about 80 dB with respect to the SNR at the receiver site. First, we investigate the effect of the power allocation factor ρ in (12) on the BER performance under fixed power allocation. To this end, Fig. 3 shows the average BER and the individual BER for

$$\Pr_{e_{m\to k|s_m=0}} = \int_{\frac{1}{2}\gamma h_k P_m}^{\infty} \mathcal{N}_{y_k}\left(\gamma h_k\left(\Upsilon + \sum_{i=m+1}^{N} P_i s_i\right), \sigma_n\right) dy_k. \tag{22}$$

$$\Pr_{e_{m\to k|s_m=1}} = \int_{-\infty}^{\frac{1}{2}\gamma h_k P_m} \mathcal{N}_{y_k}\left(\gamma h_k\left(P_m + \Upsilon + \sum_{i=m+1}^{N} P_i s_i\right), \sigma_n\right) dy_k. \tag{23}$$

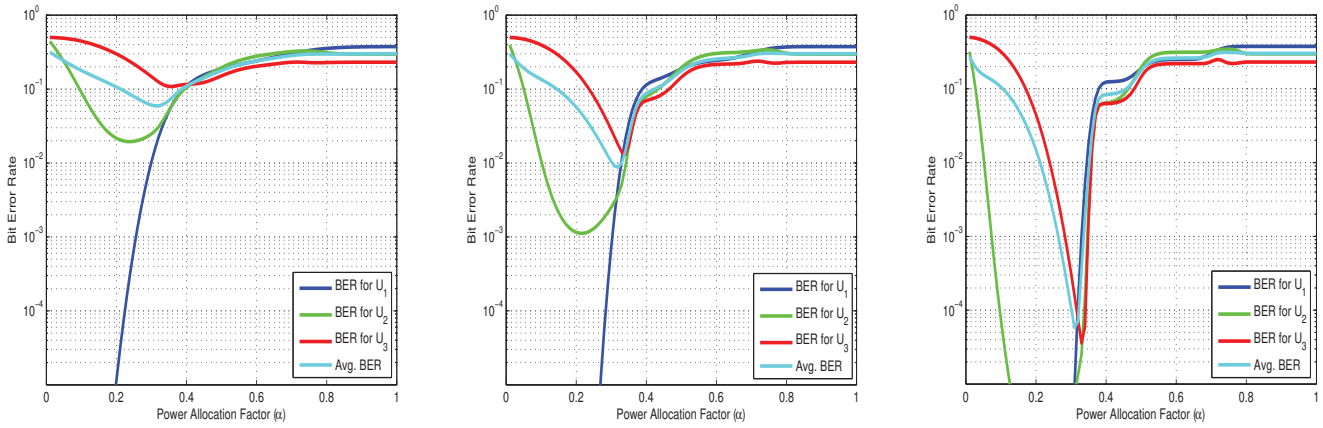

(a) (b) (c)

Figure 3: BER performance under fixed power allocation (a) SNR=110 dB, (b) SNR=115 dB and (c) SNR=120 dB.

Table I: Simulation Parameters

Description	Notation	Value
LED power	P_{LED}	0.25 W
Transmitter semi-angle	φ_i	50 deg
FOV of the PDs	ϕ_{c_i}	45 deg
Physical area of PD	A_i	1.0 cm^2
Refractive index of PD lens	n	1.5
Gain of optical filter	$T_s(\phi_{li})$	1.0
Total number of users	N	3
Channel gain of U_1	h_1	0.2835×10^{-4}
Channel gain of U_2	h_2	0.4787×10^{-4}
Channel gain of U_3	h_3	0.5272×10^{-4}

the three users versus ρ for transmit SNR values of 110 dB, 115 dB and 120 dB, respectively. It is shown that the user in the first decoding order, i.e., U_1, has low error rate compared to other users despite the poor channel conditions. This is because the signal intended for this user is transmitted with a high power compared to other signals, in order to enable U_1 to directly decode its signal of interest regardless of the interference it receives. Moreover, the best average BER performance for all users can be achieved at about $\rho = 0.3$, as in this value, the power levels allocated to users experiencing low channel gains are sufficiently high to enable correct signal decoding. As ρ increases, users with good channel conditions receive with higher power levels, which in turn reduces the power associated with the signals of the other users. As a consequence, high errors occur in the early stages of SIC decoding, and are then inherited to the following stages, which ultimately leads to poor BER performance. It is noted that for the rest of the results in this Section, $\rho = 0.3$ is considered.

Next, we validate the BER expression derived in Section III. To this end, Fig. 4 illustrates the BER performance of the three users. It is shown that the derived analytic results are in excellent agreement with the respective results from Monte Carlo simulations. It is evident that the user with the lowest decoding order exhibits the best BER performance, while the performance degrades as the decoding order increases. Yet, all users exhibit satisfactory performance above transmit SNR of 120 dB, which corresponds to receive SNR of about 40 dB and is a typical range in realistic VLC-based transmissions.

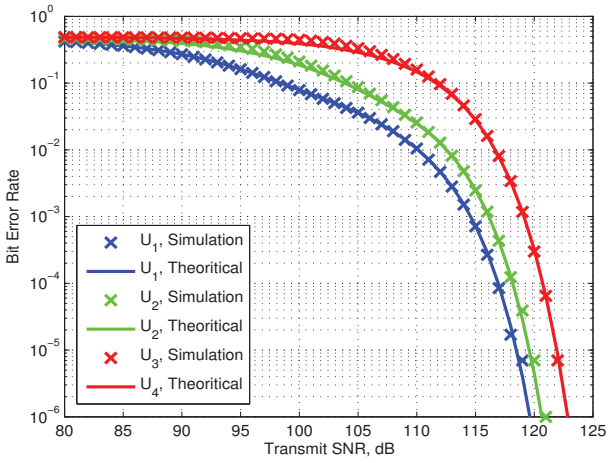

Figure 4: BER Performance with Perfect CSI.

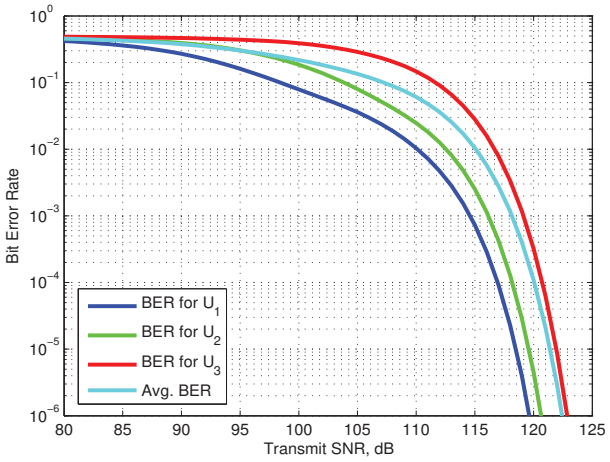

(a)

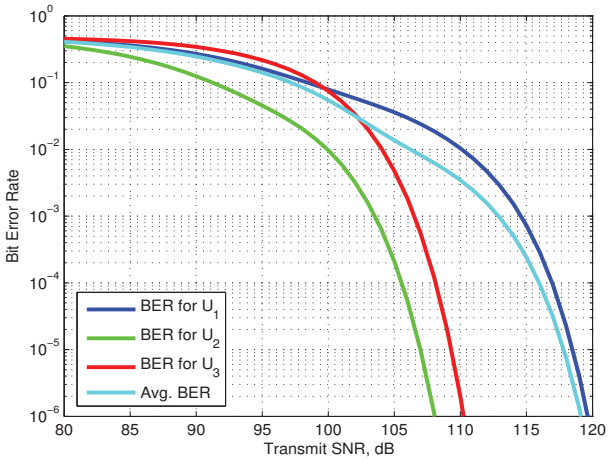

(b)

Figure 5: BER Performance with (a) fixed FOVs and (b) tunable FOVs.

Next, we investigate the effect of changing the FOVs of the users on the overall system performance. As shown in (2), the optical concentrator gain can be enhanced by reducing the FOV. Thus, we can utilize FOV tuning in order to increase the differences between the path gains of the different users, which is favorable in the context of NOMA. To this end, we assume that the PDs have tunable FOVs that can be adjusted to one of two possible settings, i.e., $FOV1 = 45^o$ and $FOV2 = 20^o$. The adjustment of the FOV depends on the user location with respect to the LED, such that the lower setting is chosen if it allows a LOS link between the PD and the transmitting LED. Fig. 5 shows the BER performance of the three users under two different scenarios: a) fixed FOVs, where the FOV is always adjusted to 45^o, and b) tunable FOVs, where the FOV of each PD is tuned according to its location. It is observed that the BER performance of U_2 and U_3 enhances dramatically when the tunable FOVs strategy is implemented. This is because smaller FOVs sare utilized leading to an enhancement in the PDs' gain which in turn boosts the received SNR at the user terminals. It can also be noticed that the performance of U_1 remained the same, which implies that the FOV of this user was adjusted to the larger FOV value due to its location. Based on the above, it becomes evident that FOVs' tuning is beneficial for enhancing the average BER performance of NOMA-based systems.

V. Conclusions

The present work was devoted to the analysis of the BER performance in a downlink VLC network where multiple access was provided by means of the recently introduced NOMA method. A novel analytic expression is derived for the BER of the considered set up, which is rather generic as it accounts for any number of users and takes into consideration the cancellation errors and the interference inherit in the involved SIC process. Respective Monte Carlo simulations were provided for verifying the validity of the derived analytical results, which were subsequently used for analyzing the performance of NOMA-based VLC systems. This led to useful insights that can be particularly helpful in future design and deployments of VLC systems. For example, it was shown that tuning the FOVs of the PDs can add a new degree of freedom in enhancing the channel gain differences among users, leading to a remarkable performance gain compared to conventional approaches.

References

[1] P. H. Pathak, X. Feng, P. Hu, and P. Mohapatra, "Visible light communication, networking, and sensing: A survey, potential and challenges," *Commun. Surveys Tuts.*, vol. 17, no. 4, pp. 2047–2077, Fourthquarter 2015.

[2] D. Karunatilaka, F. Zafar, V. Kalavally, and R. Parthiban, "LED based indoor visible light communications: State of the art," *Commun. Surveys Tuts.*, vol. 17, no. 3, pp. 1649–1678, Aug. 2015.

[3] H. Marshoud, V. M. Kapinas, G. K. Karagiannidis, and S. Muhaidat, "Non-orthogonal multiple access for visible light communications," *IEEE Photon. Technol. Lett.*, vol. 28, no. 1, pp. 51–54, Jan. 2016.

[4] L. Yin, X. Wu, and H. Haas, "On the performance of non-orthogonal multiple access in visible light communication," in *Proc. IEEE 26th Annual International Symposium on Personal, Indoor, and Mobile Radio Communications (PIMRC)*, Aug. 2015, pp. 1354–1359.

[5] L. Yin, W. O. Popoola, X. Wu, and H. Haas, "Performance evaluation of non-orthogonal multiple access in visible light communication," *IEEE Trans. Commun.*, vol. 64, no. 12, pp. 5162–5175, Dec. 2016.

[6] R. C. Kizilirmak, C. R. Rowell, and M. Uysal, "Non-orthogonal multiple access (NOMA) for indoor visible light communications," in *Proc. 4th International Workshop on Optical Wireless Communications (IWOW)*, Sep. 2015, pp. 98–101.

[7] Z. Ding, Z. Yang, P. Fan, and H. Poor, "On the performance of non-orthogonal multiple access in 5G systems with randomly deployed users," *IEEE Signal Process. Lett.*, vol. 21, no. 12, pp. 1501–1505, Dec. 2014.

[8] "IEEE standard for local and metropolitan area networks–part 15.7: Short-range wireless optical communication using visible light," *in IEEE Std 802.15.7-2011*, pp. 1–309, Sep. 6 2011.

[9] F. Miramirkhani and M. Uysal, "Channel modeling and characterization for visible light communications," *IEEE Photon. J.*, vol. 7, no. 6, pp. 1–16, Dec. 2015.

[10] I. Moreno and C.-C. Sun, "Modeling the radiation pattern of LEDs," *Opt. Express*, vol. 16, no. 3, pp. 1808–1819, Feb. 2008. [Online]. Available: http://www.opticsexpress.org/abstract.cfm?URI=oe-16-3-1808

[11] T. Komine and M. Nakagawa, "Fundamental analysis for visible-light communication system using LED lights," *IEEE Trans. Consum. Electron.*, vol. 50, no. 1, pp. 100–107, Feb. 2004.

[12] L. Dai, B. Wang, Y. Yuan, S. Han, C. l. I, and Z. Wang, "Non-orthogonal multiple access for 5G: solutions, challenges, opportunities, and future research trends," *IEEE Commun. Mag.*, vol. 53, no. 9, pp. 74–81, Sep. 2015.